

Improved signal stability from a laser vaporization source with a liquid metal target

Colleen M. Neal, Gary A. Breaux, Baopeng Cao, Anne K. Starace, and Martin F. Jarrold^{a)}
Department of Chemistry, Indiana University, 800 East Kirkwood Avenue, Bloomington, Indiana 47405

(Received 16 April 2007; accepted 31 May 2007; published online 13 July 2007)

The translating and rotating rod or disk of a conventional laser vaporization cluster source is replaced by a liquid metal target. The self-regenerating liquid surface prevents cavities from being bored into the sample by laser ablation. The laser beam strikes a near pristine surface with each pulse, resulting in signals with much better short and long term stabilities. While this approach cannot be used for refractory metals such as tungsten and molybdenum, it is ideal for studies of bimetallic clusters, which can easily be prepared by laser vaporization of a liquid metal alloy.

© 2007 American Institute of Physics. [DOI: [10.1063/1.2751393](https://doi.org/10.1063/1.2751393)]

INTRODUCTION

It is well established that properties change as one moves from the macroscopic world to the nanometer size regime. At the small end of this size range are atomic clusters containing less than 500 atoms. In the cluster size regime, properties often change abruptly with the addition or removal of a single atom. The geometries can be quite different from the bulk because the surface atoms become more numerous than internal atoms. It is in this size regime that many of the properties we normally associate with bulk materials first emerge, so it is important to gain a broad understanding of how clusters behave thermodynamically, electronically, and optically. In addition to these more fundamental questions, there is an interest in the applications of atomic clusters in catalysis and in the development of new materials.

Metal clusters are usually generated by either an oven-based source or a laser vaporization source. The former uses high temperature to vaporize a material into a buffer gas, which is then cooled to promote the growth of clusters by aggregation in the gas phase. This approach has been used extensively for low boiling point materials such as sodium.¹⁻³ However, it becomes technically difficult to implement for more refractory materials because of the need for extensive heat shielding and careful material choices.⁴⁻⁶ Perhaps the pinnacle of this effort is represented by the work of Riley *et al.* who constructed an oven source capable of generating relatively large clusters from more refractory metals such as chromium, nickel, copper, aluminum, and silver.⁷ In the early 1980s this approach was largely usurped by the development of a laser vaporization source by Smalley and collaborators.^{8,9}

A laser vaporization source uses a laser to vaporize a solid target into a flowing buffer gas. The advantage of this approach is that only a small area of the target is heated by the pulsed laser, avoiding all the complications associated with a high temperature oven. During the laser pulse, the

vaporized material forms a plasma, which is then entrained in a flowing buffer gas where it cools and recombines. The vaporized atoms then condense to form clusters. A problem with this approach is that if the laser is fired continuously at the same spot, it bores a small hole and the signal intensity decreases as the material is no longer ejected into the buffer gas. Smalley's solution to this problem was to use a rotating and translating rod to substantially extend the useful lifetime of the target. Several groups have described improvements to the basic source design. These refinements have been mainly directed towards providing more effective thermalization and to lowering the temperature of the clusters before they leave the source.¹⁰⁻¹²

The signal obtained from a laser vaporization source can be erratic. The laser bores a groove into the target, and signal intensity fluctuations arise if the laser hits a slightly different position in the groove. In our studies, we found the signal from a gallium target to be particularly prone to fluctuations, varying by many orders of magnitude as the target rotated. While a fluctuating signal is not a serious concern for some experiments, it can be for others. In particular, we have developed a method to measure the heat capacities of size-selected clusters based on measuring the shift in the cluster's dissociation threshold with temperature.^{13,14} Fluctuations in the signal intensities cause significant errors in the location of the dissociation threshold. To overcome this problem we developed a laser vaporization source that employs a liquid metal target where the self-regeneration of the liquid surface ensures that the laser does not dig a hole into the target. We found the short and long term stabilities to be a great improvement over those obtained using a traditional laser vaporization source with a rotating and translating target. While this source cannot be used with very refractory materials, it avoids the use of complicated motor assemblies to rotate and translate the target.

The liquid metal laser vaporization source also provides a particularly convenient approach to study alloy clusters. The study of mixed metal clusters is emerging as an important research area, but they are difficult to make. In early studies, mixed metal clusters were generated by photolysis of

^{a)}Electronic mail: mjf@indiana.edu

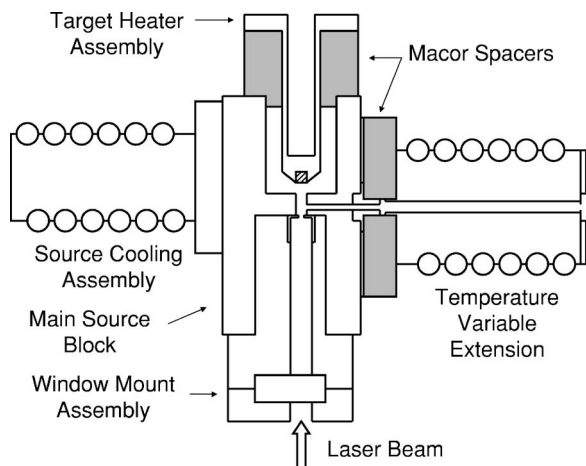


FIG. 1. Schematic diagram of the liquid metal laser vaporization source. In the figure the source is equipped with the low temperature target heater assembly and the low temperature extension.

organometallic complexes in a laser vaporization source.¹⁵⁻¹⁷ More recently, they have been prepared by laser vaporization of an alloy rod¹⁸ and from targets generated by mixing and pressing metal powders.¹⁹ There are drawbacks with both approaches: alloy rods are difficult to obtain and generally limited to a few compositions; pressed metal powder targets allow a wide range of compositions, but the large surface area of the powders makes this approach prone to contamination. The preferred method for generating mixed metal clusters has been the use of a dual rod source where two different metal rods are vaporized with different laser beams.²⁰⁻²² Some control over the cluster composition can be obtained by adjusting the pulse energy and position of the vaporization lasers. However, it is even more difficult to obtain a stable signal with a dual rod source than with a regular laser vaporization source.

SOURCE DESIGN

Figure 1 shows a schematic diagram of the source viewed from above. The source block is made from beryllium copper. The source block is cooled by the source cooling assembly that is attached at the rear of the source. The source cooling assembly is cylindrical and wrapped with copper tubing that is soldered into a groove. The temperature of the source block is measured by a *K*-type thermocouple, and a microprocessor-based temperature controller regulates the temperature of the source block to within a few degrees of the set point by controlling liquid nitrogen flow through the copper coil with a solenoid valve. The temperature of the main source block is usually maintained at around 273 K. The source is shown in Fig. 1, equipped with a low temperature target heater assembly that is suitable for low melting point materials such as gallium, tin, and their alloys. The low temperature target heater assembly is made from stainless steel, and it is heated by means of a 3/8 in. diameter cartridge heater that is placed in the hole at the back of the assembly. The temperature is measured with a *K*-type thermocouple and regulated with a microprocessor-based temperature controller. The liquid metal target, which is repre-

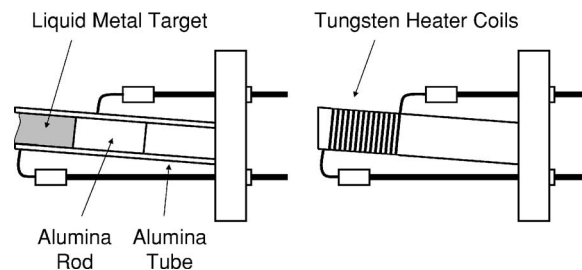


FIG. 2. Schematic diagram of the high temperature liquid metal sample holder. The view on the left hand side shows a cross section.

sented by the cross-hatched area in the figure, is located in a 0.1875 in. diameter by 0.25 in. deep hole. The sample is heated to slightly above the bulk melting point to ensure that the target remains liquid throughout the experiment. Capillary action prevents the liquid metal from dripping out.

The source uses a continuous flow of helium buffer gas that enters the main source block in the volume around the target heater assembly. The use of a continuous flow instead of a pulsed buffer gas flow provides a more stable signal by avoiding fluctuations induced by pulse to pulse variations in the gas flow from a pulsed valve. However, this benefit comes at the expense of significantly larger pumps. The helium flows around the liquid metal target and down the channel into the temperature variable extension. Another gas line is used to measure the pressure in the source. With a typical helium flow of around 350 SCCM (SCCM denotes cubic centimeter per minute at STP), the pressure is around 15 Torr when the temperature variable extension is at room temperature. The laser beam enters the source through a UV-grade fused silica window. It is focused onto the liquid metal target using a 500 mm focal length lens mounted outside the vacuum chamber. A Compex 110 excimer laser (Lambda Physik) operating at 351 nm (XeF) and 100 Hz is used as the vaporization laser. The source generates neutral clusters as well as both positively and negatively charged cluster ions, the charge resulting from the plasma generated by the vaporization laser.

To generate clusters of more refractory metals such as aluminum, which has a melting point of 933 K, a high temperature liquid metal sample holder is employed. The high temperature sample holder is shown schematically in Fig. 2. It consists of a ceramic tube (0.25 in. inner diameter) that is mounted on a stainless steel rod. The stainless rod and ceramic tube are tilted at an angle of 8° from horizontal. The purpose of this incline is to prevent the liquid metal target from dripping out of the holder: the diameter of the alumina tubing is too large for capillary action to always hold the sample in place. A short length of alumina rod separates the liquid metal target from the stainless steel rod on the base. The metal sample is heated by means of a tungsten coil wrapped around the ceramic tube (see Fig. 2). For aluminum, a heater current of around 13 A is employed. The temperature is monitored by simply looking at the sample through the window that admits the laser beam into the source. We found it fairly easy to judge the shade of orange-red emission that indicates a temperature above the melting point of alu-

minum. If the target is solid, the cluster signal only survives for a short period of time as the laser bores a hole into the target.

After formation, the clusters are carried into a temperature variable extension where their temperature is set before they leave the source. In our application, the source is used to generate cluster ions for studies of their phase transitions. These studies are performed by determining the dissociation thresholds of size-selected clusters as a function of their temperature. The change in the dissociation threshold with temperature provides a measure of the change in the internal energy with temperature, which is the heat capacity. A spike in the heat capacity due to the latent heat is the signature of a phase transition. It is critical for these measurements that the clusters are in thermal equilibrium with the walls of the extension. To determine if the clusters achieve thermal equilibrium, a series of measurements were performed, where we changed the length of the extension and changed the size of the apertures at the entrance and exit of the extension. These studies indicate that the clusters achieve thermal equilibrium under our conditions. We employ two extensions, both 10 cm long. The high temperature version (300–1200 K) incorporates heat shields and is heated by a Thermocoax heater. The heater (2 mm diameter and 4 m long) is embedded in a groove that runs around the circumference of the extension. The low temperature version (77–600 K) incorporates a cooling coil for liquid nitrogen and a shorter Thermocoax heater (2 m long) for gentle heating. The temperature of the extensions is measured by a *K*-type thermocouple, and the temperature is regulated by a microprocessor-based temperature controller. The temperature is held to better than ± 2 K.

PERFORMANCE

The liquid metal laser vaporization source is incorporated into an apparatus to measure heat capacities of size-selected clusters. After the ions exit the source they are focused into a quadrupole mass spectrometer, where a particular cluster size is selected. The size-selected clusters are then focused into a high-pressure collision cell, where some of them will fragment if their initial kinetic energy is high enough. The fragments and undissociated ions are analyzed by a second quadrupole mass spectrometer and then detected with a collision dynode and microchannel plates. Figure 3 shows a mass spectrum measured for aluminum cluster anions generated by the liquid metal laser vaporization source. To measure this spectrum the first quadrupole was set to transmit all ions, and the kinetic energy into the collision cell was set to a low value to avoid dissociation. The spectrum was measured by scanning the second quadrupole. The dominant peak in the spectrum is due to Al_{45}^+ . Note the almost complete absence of oxide impurities. Oxide impurities such as Al_nO^- and Al_nO_2^- are a common problem with aluminum clusters. Their absence here indicates that the hot aluminum surface can be kept free of oxide. The bell-shaped intensity distribution evident in Fig. 3 is a consequence of the transmission efficiency through the rest of the apparatus. For the mass spectrum shown in Fig. 3 the signal was tuned up by focusing on clusters near the center of the

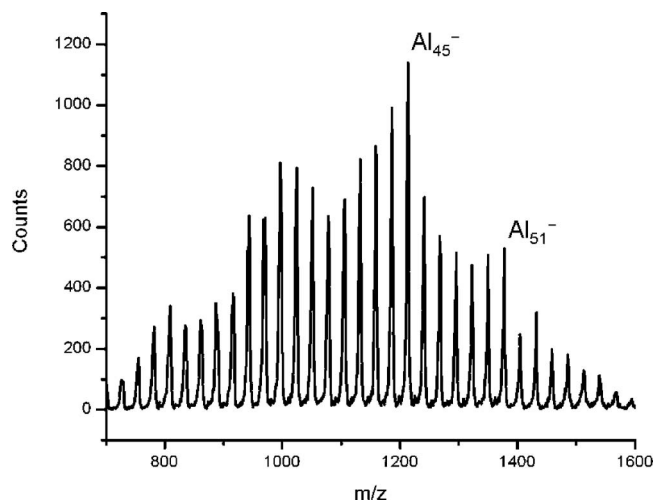


FIG. 3. Mass spectrum for aluminum cluster anions generated by the liquid metal laser vaporization source.

distribution. If, instead, the cluster signal is maximized by focusing on a higher or lower mass, a similar bell-shaped distribution is obtained, but its center is shifted to a higher or lower mass.

The long and short term stabilities of the liquid metal laser vaporization source were investigated by recording the cluster ion signal in a multichannel scaler (MCS) as a function of time. Figure 4 presents a typical trace showing the short term stability. The plot shows the signal intensity recorded for Al_{45}^+ as a function of time over a 450 ms period. For these measurements, the first quadrupole was set to transmit all ions, and the second was set to transmit the ion of interest. The plot shown in Fig. 4 is a single MCS scan recorded with a channel width of 1 ms. The peaks that occur every 10 ms are due to the signal from individual laser pulses. The root mean square fluctuation in the amplitude of the signal (the standard deviation) is 8.5%. Fluctuations in the signal intensity evident in Fig. 4 are thought to arise mainly from the shot-to-shot variations in the laser pulse

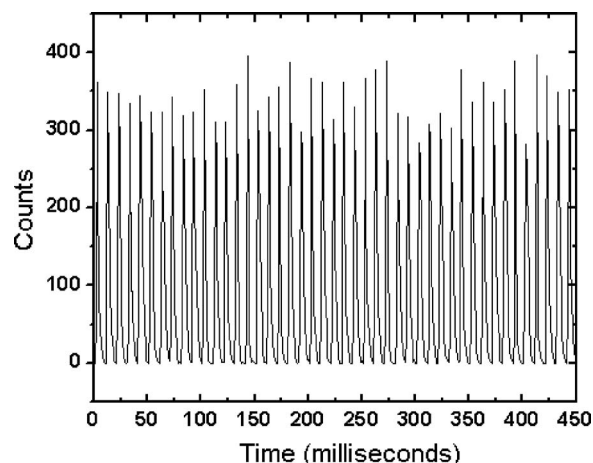


FIG. 4. A plot illustrating the short term stability of the liquid metal laser vaporization source. The plot shows the signal intensity recorded for Al_{45}^+ as a function of time over a 450 ms period. The peaks in the intensity every 10 ms result from the individual laser pulses.

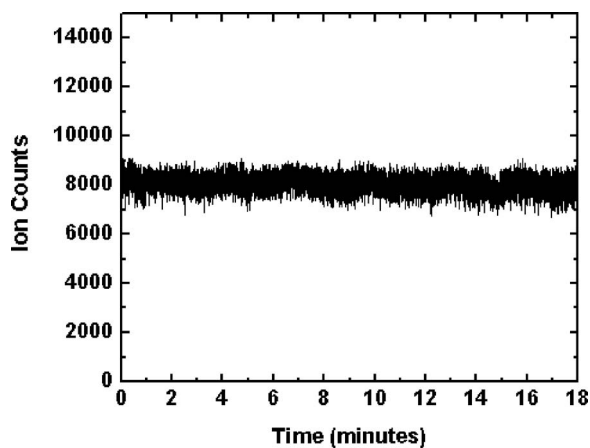


FIG. 5. A plot illustrating the long term stability of the signal from the liquid metal laser vaporization source. The plot shows the signal intensity recorded for Al_{45}^+ as a function of time over an 18 min period.

energy. Figure 5 shows a plot of the signal intensity recorded with a channel width of 70 ms over a longer time period (18 min).

The average signal resulting from each laser pulse in Fig. 4 is 850 ions, which corresponds to 85 000 ions/s with a 100 Hz laser. For these measurements, the ions were transmitted through two quadrupole mass spectrometers and a collision cell before being detected. The temperature variable extension attached to the source also significantly reduces the cluster ion signal. So, the signals generated directly by the source are much larger than the values reported above. The signal intensity obtained with the liquid metal source is at least as good as that obtained with a conventional laser vaporization source, under similar conditions.

As noted above, the liquid metal laser vaporization source is particularly well suited to investigating mixed metal clusters. To date we have used the source to investigate gallium-rich gallium/aluminum alloys, which melt at a low temperature (below 303 K), tin-rich tin/copper alloys,²³ and aluminum-rich aluminum/copper alloys, which melt at a high temperature. The gallium/aluminum alloys were prepared by melting the gallium sample in the low temperature liquid metal sample holder in air and mixing in aluminum flakes to the required composition. The sample holder was then placed in a refrigerator to freeze the target before installing it into the apparatus (gallium is notorious for supercooling). The aluminum/copper alloys were prepared by heating copper shot and an aluminum rod in a 1/4 in. diameter ceramic tube in a diffusion pumped vacuum line for more than 24 h. After cooling the samples were removed from the ceramic tube, and an appropriate length was cut off and installed into the high temperature liquid metal sample holder.

Figure 6 shows mass spectra recorded for an aluminum/copper alloy containing 25 at. % copper. The spectrum is complex. The asterisks are placed over peaks that are believed to be predominantly pure Al_n^- . Larger peaks, at around 10 Da higher in mass than the peaks assigned to the pure Al_n^- clusters, are attributed to predominantly $\text{Al}_{n-2}\text{Cu}^-$. The average atomic mass of copper (63.546 g mol⁻¹) is more than twice the average atomic mass of aluminum (26.981 g mol⁻¹), and so the average atomic mass of an

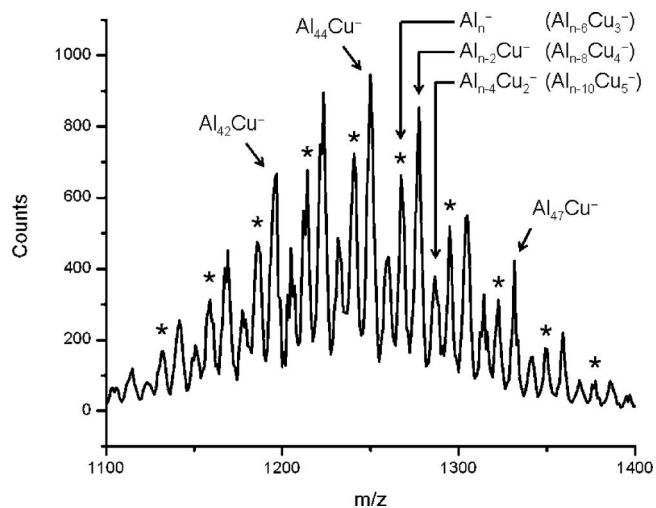


FIG. 6. Mass spectra recorded for cluster anions generated by the liquid metal laser vaporization source from a copper/aluminum alloy. The spectrum was recorded with an alloy containing 25% copper. The star symbols are located over peaks that are predominantly Al_n^- (see text).

$\text{Al}_{n-2}\text{Cu}^-$ cluster is 9.6 Da greater than that of Al_n^- . The $\text{Al}_{n-4}\text{Cu}_2^-$ cluster is another 9.6 Da higher in mass than the $\text{Al}_{n-2}\text{Cu}^-$ cluster. The next cluster in this sequence ($\text{Al}_n^-, \text{Al}_{n-2}\text{Cu}^-, \text{Al}_{n-4}\text{Cu}_2^-, \dots$) is $\text{Al}_{n-6}\text{Cu}_3^-$, which has an average mass of 1.77 Da above the mass of the Al_{n+1}^- cluster. Thus, the $\text{Al}_{n-2m}\text{Cu}_m^-$ clusters form a series of overlapping peaks separated by around 10 Da (see Fig. 6). The most intense peak in the mass spectrum shown in Fig. 6 is at around 1250 Da. This is attributed to $\text{Al}_{44}\text{Cu}^-$ with some overlapping $\text{Al}_{38}\text{Cu}_4^-$. As the copper content increases, the peaks become broader because copper has two isotopes, while aluminum has only one. The relatively narrow peaks in the spectrum shown in Fig. 6 indicate a fairly low copper content in the clusters, lower than the amount of copper present in the bulk alloy (25 at. %). Thus, the probability of incorporating copper atoms into the clusters is less in the case of aluminum atoms. Simpler mass spectra can be generated by lowering the copper concentration. For example, if the copper concentration is lowered to 2 at. %, the dominant peaks in the spectrum are due to pure aluminum cluster anions, Al_n^- , and the only other peaks present in significant abundance are those due to $\text{Al}_{n-2}\text{Cu}^-$. The $\text{Al}_{n-2}\text{Cu}^-$ peaks have intensities around 50% of the pure Al_n^- clusters.

As described above, the source described here was developed to perform heat capacity measurements on size-selected clusters. An example of the heat capacities measured for aluminum/copper alloy clusters is shown in Fig. 7. This figure shows a plot of the heat capacities measured for $\text{Al}_{55}\text{Cu}^-$. The red points are the average heat capacities measured values. The thin dashed line in Fig. 7 shows heat capacities determined from a modified Debye model that incorporates finite-size effects.²⁴ There is a sharp peak in the heat capacities for $\text{Al}_{55}\text{Cu}^-$ at 550 K, which we attribute to a melting transition. The dip in the heat capacities at around 250 K is probably due to an annealing transition, where the cluster formed at low temperature is trapped in a high energy geometry and anneals into the ground state as the temperature rises.²⁵ Annealing to a lower energy structure causes an increase in the

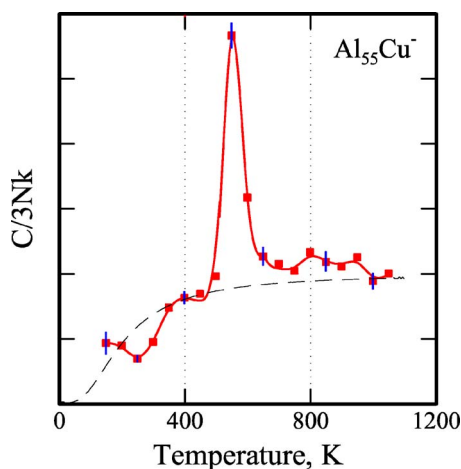


FIG. 7. Plot of the heat capacities measured for $\text{Al}_{55}\text{Cu}^-$. The red points are the average measured values. The vertical blue lines show representative standard deviations for some of the points. The thin dashed line shows heat capacities determined from a modified Debye model that incorporates finite-size effects (Ref. 21).

amount of energy required to cause dissociation, which causes an apparent dip in the heat capacity. The vertical blue lines on some of the data points in Fig. 7 show representative standard deviations. The small size of these error bars is a consequence of the stability of the signal from the liquid metal laser vaporization source.

CONCLUSIONS

We have developed a liquid metal laser vaporization source for the generation of thermalized metal clusters. The use of a liquid metal target provides signals with substantially improved short term and long term stabilities. The use of a liquid metal target is particularly useful for studies of mixed metal clusters. The source is currently being used to measure heat capacities of size-selected metal clusters.

ACKNOWLEDGMENT

The authors are grateful to the National Science Foundation for support of this work.

- ¹E. Schumacher, W. H. Gerber, H.-P. Harri, M. Hofmann, and E. Scholl, ACS Symp. Ser. **179**, 83 (1982).
- ²J. Mühlbach, E. Recknagel, and K. Sattler, Surf. Sci. **106**, 188 (1981).
- ³A. Yokozeki and G. D. Stein, J. Appl. Phys. **49**, 2224 (1978).
- ⁴C. G. Granqvist and R. A. Buhrman, J. Appl. Phys. **47**, 2200 (1976).
- ⁵D. P. Preuss, S. A. Pace, and J. L. Gole, J. Chem. Phys. **71**, 3553 (1979).
- ⁶R. S. Bowles, J. J. Kolstad, J. M. Calo, and R. P. Andres, Surf. Sci. **106**, 117 (1981).
- ⁷S. J. Riley, E. K. Parks, C. R. Mao, L. G. Pobo, and S. Wexler, J. Phys. Chem. **86**, 3911 (1982).
- ⁸T. G. Dietz, M. A. Duncan, D. E. Powers, and R. E. Smalley, J. Chem. Phys. **74**, 6511 (1981).
- ⁹R. E. Smalley, Laser Chem. **2**, 167 (1983).
- ¹⁰P. Milani and W. A. de Herr, Rev. Sci. Instrum. **61**, 1835 (1990).
- ¹¹S. Maruyama, L. R. Anderson, and R. E. Smalley, Rev. Sci. Instrum. **61**, 3686 (1990).
- ¹²J. P. Bucher, D. C. Douglass, and L. A. Bloomfield, Rev. Sci. Instrum. **63**, 5667 (1982).
- ¹³G. A. Breaux, R. C. Benirschke, T. Sugai, B. S. Kinnear, and M. F. Jarrold, Phys. Rev. Lett. **91**, 215508 (2003).
- ¹⁴C. M. Neal, A. K. Starace, and M. F. Jarrold, J. Am. Soc. Mass Spectrom. **18**, 74 (2007).
- ¹⁵K. LaiHing, P. Y. Cheng, and M. A. Duncan, J. Phys. Chem. **91**, 6521 (1987).
- ¹⁶S. M. Beck, J. Chem. Phys. **90**, 6306 (1989).
- ¹⁷Z. Y. Chen, G. J. Walder, and A. W. Castleman, Phys. Rev. B **49** 2739 (1994).
- ¹⁸O. C. Thomas, W. J. Zheng, and K. H. Bowen, J. Chem. Phys. **114**, 5514 (2001).
- ¹⁹X. P. Xing, Z. X. Tian, H. T. Liu, and Z. Tang, Rapid Commun. Mass Spectrom. **17**, 1411 (2003).
- ²⁰S. Nonose, Y. Sone, K. Onodera, S. Suda, and K. Kaya, J. Phys. Chem. **94**, 2744 (1990).
- ²¹R. L. Wagner, W. D. Vann, and A. W. Castleman, Rev. Sci. Instrum. **68**, 3010 (1997).
- ²²E. Janssens, T. Van Hoof, N. Veldeman, S. Neukermans, M. Hou, and P. Lievens, Int. J. Mass. Spectrom. **252**, 38 (2006).
- ²³G. A. Breaux, D. A. Hillman, C. M. Neal, and M. F. Jarrold, J. Phys. Chem. A **109**, 8755–8759 (2005).
- ²⁴J. Bohr, Int. J. Quantum Chem. **84**, 249 (2001).
- ²⁵G. A. Breaux, C. M. Neal, B. Cao, and M. F. Jarrold, Melting, Phys. Rev. Lett. **94**, 173401 (2005).

Review of Scientific Instruments is copyrighted by the American Institute of Physics (AIP). Redistribution of journal material is subject to the AIP online journal license and/or AIP copyright. For more information, see <http://ojps.aip.org/rsio/rsicr.jsp>